



Thermal and Exergy Analysis of an Organic Rankine Cycle Power Generation System with Refrigerant R245fa

Xinlei Zhou, Ping Cui & Wenke Zhang

To cite this article: Xinlei Zhou, Ping Cui & Wenke Zhang (2020) Thermal and Exergy Analysis of an Organic Rankine Cycle Power Generation System with Refrigerant R245fa, Heat Transfer Engineering, 41:9-10, 905-918, DOI: [10.1080/01457632.2019.1576824](https://doi.org/10.1080/01457632.2019.1576824)

To link to this article: <https://doi.org/10.1080/01457632.2019.1576824>



Published online: 27 Mar 2019.



Submit your article to this journal [↗](#)



Article views: 126



View related articles [↗](#)



View Crossmark data [↗](#)



Citing articles: 1 View citing articles [↗](#)



Thermal and Exergy Analysis of an Organic Rankine Cycle Power Generation System with Refrigerant R245fa

Xinlei Zhou^a, Ping Cui^{a,b}, and Wenke Zhang^{a,b}

^aSchool of Thermal Engineering, Shandong Jianzhu University, Jinan, China; ^bKey Laboratory of Renewable Energy Utilization Technology in Building, Ministry of Education, Jinan, China

ABSTRACT

In this paper, the performance of an organic Rankine cycle (ORC) power generating system operating with refrigerant R245fa was investigated when heat source temperature was below 200 °C. It was found the system thermal efficiency increased but the exergy efficiency of the evaporator decreased with the increase of the heat source temperature. It was also obtained that the exergy efficiency of the evaporator could reach 70% when the heat source temperature was 80 °C, which was high enough to prove that the transformation efficiency between the waste heat and the electricity power was ideal. In the simulation model, the area of different parts of the heat exchanger were considered to be varied, flow rate of the waste heat and working medium, the system thermal and exergy efficiency of the evaporator were respectively calculated, the different parameter change regarding the performance influences of the ORC system were simulated. The results can be considered as a reference to research on the design of ORC power generating systems and heat exchangers.

Introduction

Due to the excessive fuel consumption and environmental pollution, energy saving and emission reduction technologies have become urgently needed worldwide. In recent years, more attention has been paid to the studies in terms of the organic Rankine cycle (ORC) generation system by means of the low-grade heat sources, such as the industrial waste water, exhaust gas and solar energy in order to reduce the fossil fuel consumption and the pollution during the conventional thermal power generation [1–4]. The existing research regarding the ORC system is mainly focused on the working medium selection [5–9] and the system optimization [10–15].

Compared with the Clausius–Rankine steam power plant, the ORC system can use a relatively lower grade heat source. Many researchers focused on the studies in terms of the influence of different evaporating temperatures on the system performance. Sung et al. [16] developed an ORC system with R245fa refrigerant. In this study, a flue–gas heat–recovery heat exchanger with the maximum heat transfer rate of 1900 kW was designed for the waste heat source with a high

temperature of over 260 °C. The system produced 105.8 kW with a thermal efficiency of 8.6%. Miao et al. [17] conducted some experiments by adjusting two independent parameters: the pumping frequency of the circulating pump for the working medium R123 and the shaft torque of the expander. The maximum shaft power and the thermal efficiency were measured to be 2.35 kW and 6.39% at the heat source temperature of 140 °C, but they were 3.25 kW and 5.12% at the heat source temperature of 160 °C. Fu [18] investigated the effect of off-design heat source temperature on the heat transfer characteristics by a pressure control approach. It was found in this study a heat source temperature variation of –10.3 °C resulted in variations of –13.6% in the quantity of net power output and –11.5% system thermal efficiency respectively; and a source temperature variation of +19.8 °C resulted in +22.6% variation in the quantity of net power output and +17.4% variation of system thermal efficiency, respectively.

In this work, a mathematical model has been developed to analyze the thermal influences of the heat source temperature, mass flow rate of the working fluid and the evaporator heat transfer area on the system

Nomenclature

C_p	Specific heat capacity at constant pressure, $\text{J} \cdot (\text{kg} \cdot \text{K})^{-1}$	ρ	Density, $\text{kg} \cdot \text{m}^{-3}$
D	Characteristic diameter of the pipe, m	v	Velocity, $\text{m} \cdot \text{s}^{-1}$
E	Exergy rate, kW	ζ	Coefficient of mechanical efficiency
e	Specific exergy, $\text{kJ} \cdot \text{kg}^{-1}$	Subscripts	
F	Area, m^2	a	ORC working medium
GWP	Global warming potential	b	Heat source
h	Specific enthalpy, $\text{kJ} \cdot \text{kg}^{-1}$	evap	Evaporator
K	Heat transfer coefficient, $\text{W} \cdot \text{m}^{-2} \cdot \text{K}^{-1}$	ex	Exergy
m	Flow rate, $\text{kg} \cdot \text{s}^{-1}$	f	Working medium during the evaporating area
ODP	Ozone depletion potential	i	Inlet of any relevant component
ORC	Organic Rankine cycle	in	Inside
Pr	Prandtl number	j	Preheater
p	Pressure, Pa	k	superheater
Q	Heat transfer rate, kW	o	Outlet of any relevant component
Re	Reynolds number	out	Outside
s	Specific entropy, $\text{kJ} \cdot (\text{kg} \cdot \text{K})^{-1}$	pump	Working medium pump.
T	Temperature, $^{\circ}\text{C}$	r	Working medium during the preheating area or the superheating area
v	Specific volume, $\text{m}^3 \cdot \text{kg}^{-1}$	s	Saturation
W	Power, kW	surr	Reference environment condition
x	Vapor quality	tur	Turbine expander
Greek Symbols		th	Thermal
α	Convective heat transfer coefficient, $\text{W} \cdot \text{m}^{-2} \cdot \text{K}^{-1}$	Superscripts	
η	Efficiency, %	-	The average of any quantity
λ	Heat conductivity, $\text{W} \cdot \text{m}^{-1} \cdot \text{K}^{-1}$		
μ	Dynamic viscosity, $\text{Pa} \cdot \text{s}$		

performance, which could be a recommendation for the design of a component or the ORC system.

Physical models

The ORC system functions similarly to a Clausius–Rankine steam power plant, but instead uses an organic working fluid such as R245fa, the evaporation temperature of which is much lower than the water under the same pressure [19]. As shown in Figure 1, the fluid medium firstly absorbs enough heat from the heat source in the evaporator and evaporates into gas with high pressure and high temperature, then gas state medium flows into the expander and releases the thermal energy which can be transformed into electric power by the generator working together with the expander. With a high pressure drop and temperature drop in the expander, the working medium then flows into the condenser and condenses into the liquid by the cooling water. After being compressed by the medium pump, working medium enters the evaporator again, which means a whole generation cycle is accomplished [20]. The T–S diagram of the ORC system is illustrated in Figure 2. In addition, R245fa is applied as the working medium in the model of ORC power generating system model

and some relative properties about R245fa are listed in Table 1.

Mathematical model

In order to simplify the calculation, some assumptions and details for the system are proposed as follows:

1. The entire system is in a steady operation and there is no heat losses from the system to the ambient environment.
2. The temperature and pressure during the condenser and evaporator are assumed to be constant.
3. The evaporation temperature should not be higher than 426.15 K, which is the critical temperature of R245fa.
4. The evaporator is divided into preheating area, evaporating area and super-heating area.
5. The specific heat capacity of the heat source is considered to be constant.
6. The ambient temperature is assumed to be constant at 25 $^{\circ}\text{C}$.
7. The torque efficiencies of the expander and working medium pump are both assumed to be 80%.

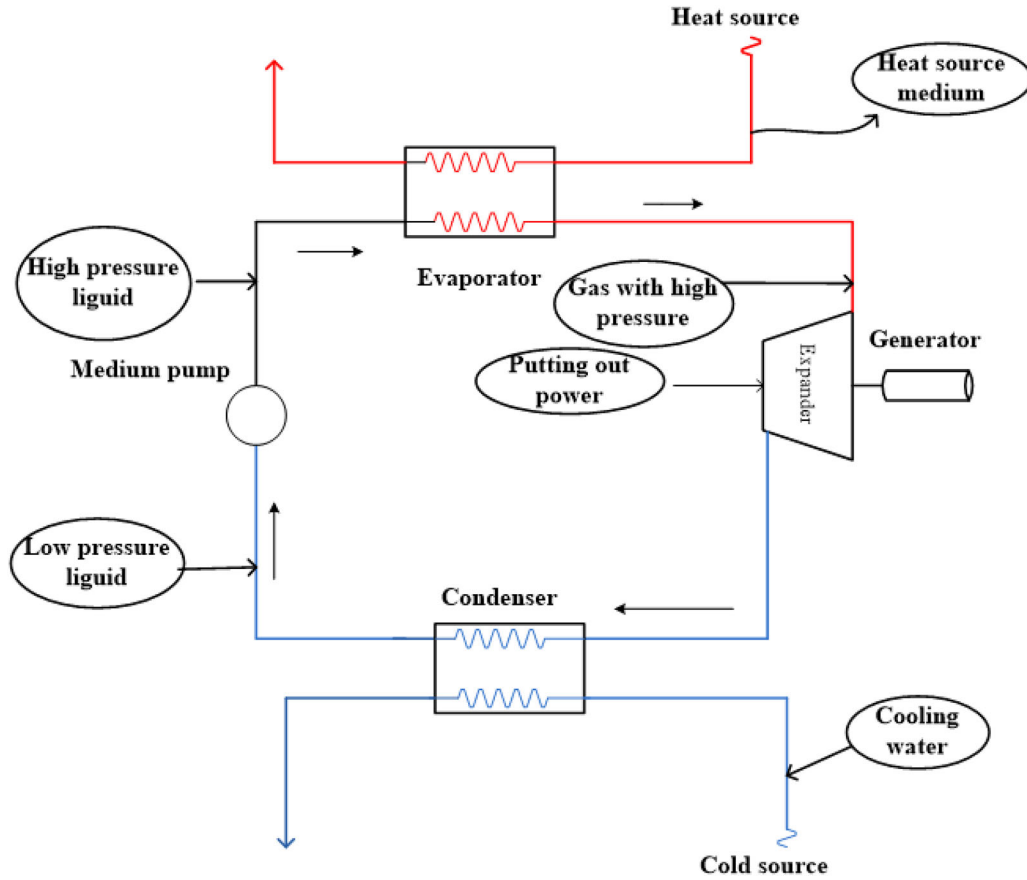


Figure 1. Working process of the ORC power generating system.

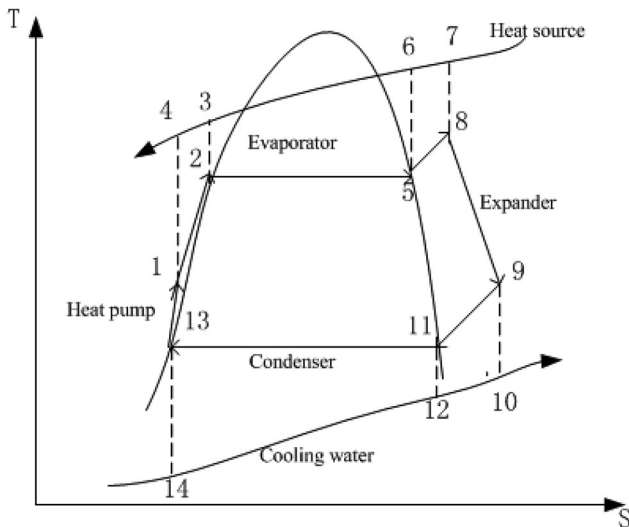


Figure 2. T-S diagram of the ORC power generating system.

Based on the aforementioned assumptions, the heat source fluid convective heat transfer coefficient is achieved by [21]:

$$\alpha_b = 0.023 \text{Re}_b^{0.8} \text{Pr}_b^{0.4} \lambda_b / D_b \quad (1)$$

where, $\text{Re} = \rho \cdot v \cdot D / \mu$ and $\text{Pr} = C_p \cdot \mu / \lambda$ are the Reynolds and Prandtl numbers of the working fluid

respectively, within the range of $\text{Re} > 10^5$ and $0.6 < \text{Pr} < 60$.

$$\alpha_{a,f} = 0.023 \lambda_{a,f} \left(1.8 / (1/x - 1) \right)^{0.64} (\rho_{a,f} / \rho_s)^{0.4} \text{Re}_{a,f}^{0.8} \text{Pr}_{a,f}^{0.4} / D_a \quad (2)$$

For the working medium during the evaporating area, its convective heat transfer coefficient is calculated by [21]:

For the working medium during the preheating area and superheating area, the convective heat transfer coefficient is expressed as follows:

$$\alpha_{a,r} = 0.023 \text{Re}_{a,r}^{0.8} \text{Pr}_{a,r}^{0.4} \lambda_{a,r} / D_a \quad (3)$$

In order to simply the calculation, the scaling factor of the heat exchanger is ignored, and the coefficient of the heat transfer can be calculated as follows [22]:

$$K = \left(\frac{D_{a,\text{out}}}{D_{a,\text{in}} \alpha_a} + \frac{D_{a,\text{out}}}{2\lambda} \cdot \ln \left(\frac{D_{a,\text{out}}}{D_{a,\text{in}}} \right) + 1/\alpha_b \right)^{-1} \quad (4)$$

The energy balance between the working medium and heat source sides in each part of the evaporator can be described by Equations (5) and (6):

Table 1. Properties of the ORC working fluid R245fa.

Medium	Toxicity	Flammability	Environmental impact	Critical temperature, K	Critical pressure, MPa	Density (25 °C, kg/m ³)
R245fa	non-toxic	Nonflammable	ODP = 0, and GWP is low	427.16	3.604	1339.01

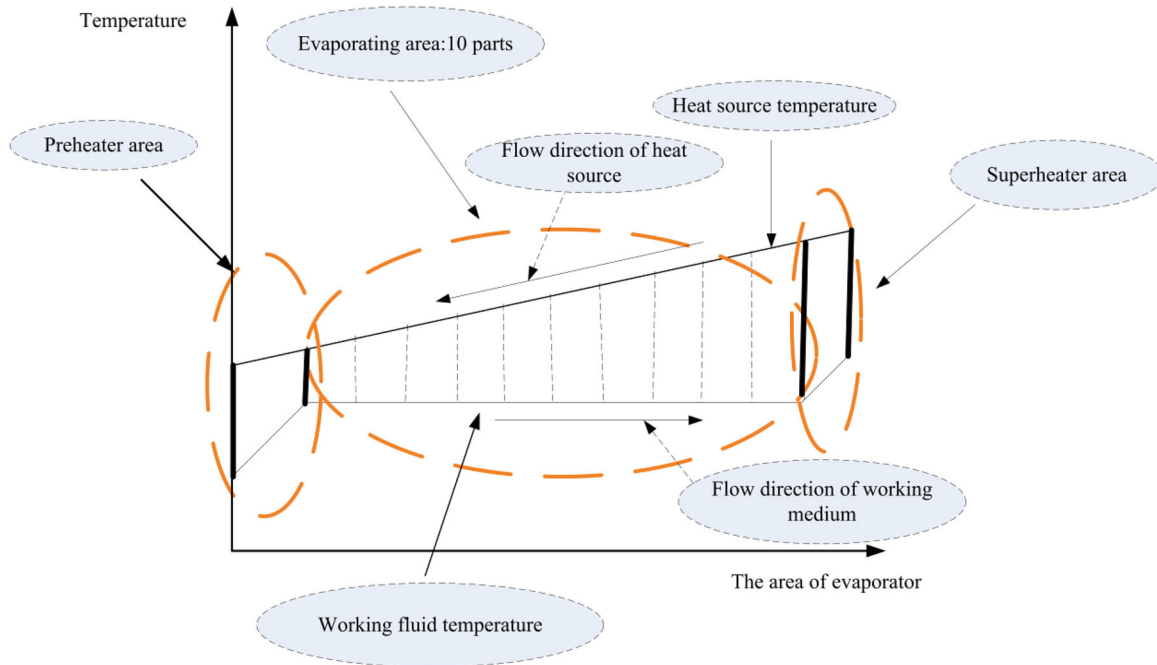


Figure 3. Heat transfer process of the evaporator.

$$C_{pb}m_b^{pb}(T_{b,i}-T_{b,o}) = m_a(h_{a,o}-h_{a,i}) \quad (5)$$

$$KF(\Delta T_o-\Delta T_i)/\ln(\Delta T_o/\Delta T_i) = C_{pb}m_b(T_{b,o}-T_{b,i}) \quad (6)$$

where ΔT is the temperature difference between the heat source and the working medium.

The heat transfer rate in the evaporator is given by:

$$Q_{evap} = m_a(h_o-h_i) \quad (7)$$

The power output of the expander and the power input of the working fluid pump can be expressed by Eqs. (7) and (8), respectively:

$$W_{tur} = \xi_{tur}m_a \int_{h_i}^{h_o} dh \quad (8)$$

$$W_{pump} = \xi_{pump}m_a \int_{p_i}^{p_o} \nu dp \quad (9)$$

$$s_o-s_i = C_{pa} \ln(T_o-T_i) \quad (10)$$

Because the pressure of working medium in superheater is constant, so the working medium entropy at outlet of the superheater can be obtained by:

The thermal efficiency of the ORC system can be achieved by:

$$\eta_{th} = (W_{tur}-W_{pump})/Q_{evap} \quad (11)$$

The working medium exergy governing equation with regard to the evaporator can be expressed as follows:

$$E_b = m_a e_o - m_a e_i + \Delta E \quad (12)$$

where e is the specific exergy of working medium in the evaporator which can be expressed as:

$$e = h-h_{surr}-T_{surr}(s-s_{surr}) \quad (13)$$

The heat source exergy in the evaporator can be expressed as [21]:

$$E_b = m_b C_{pb} \left(\bar{T} - T_{surr} - T_{surr} \ln \frac{\bar{T}}{T_{surr}} \right) \quad (14)$$

The exergy efficiency of the evaporator can be achieved by:

$$\eta_{ex} = (m_a e_o - m_a e_i) / E_b \quad (15)$$

The development of the simulation program for the evaporator

In the modeling procedure, the following parameters should be given first: the evaporator configuration

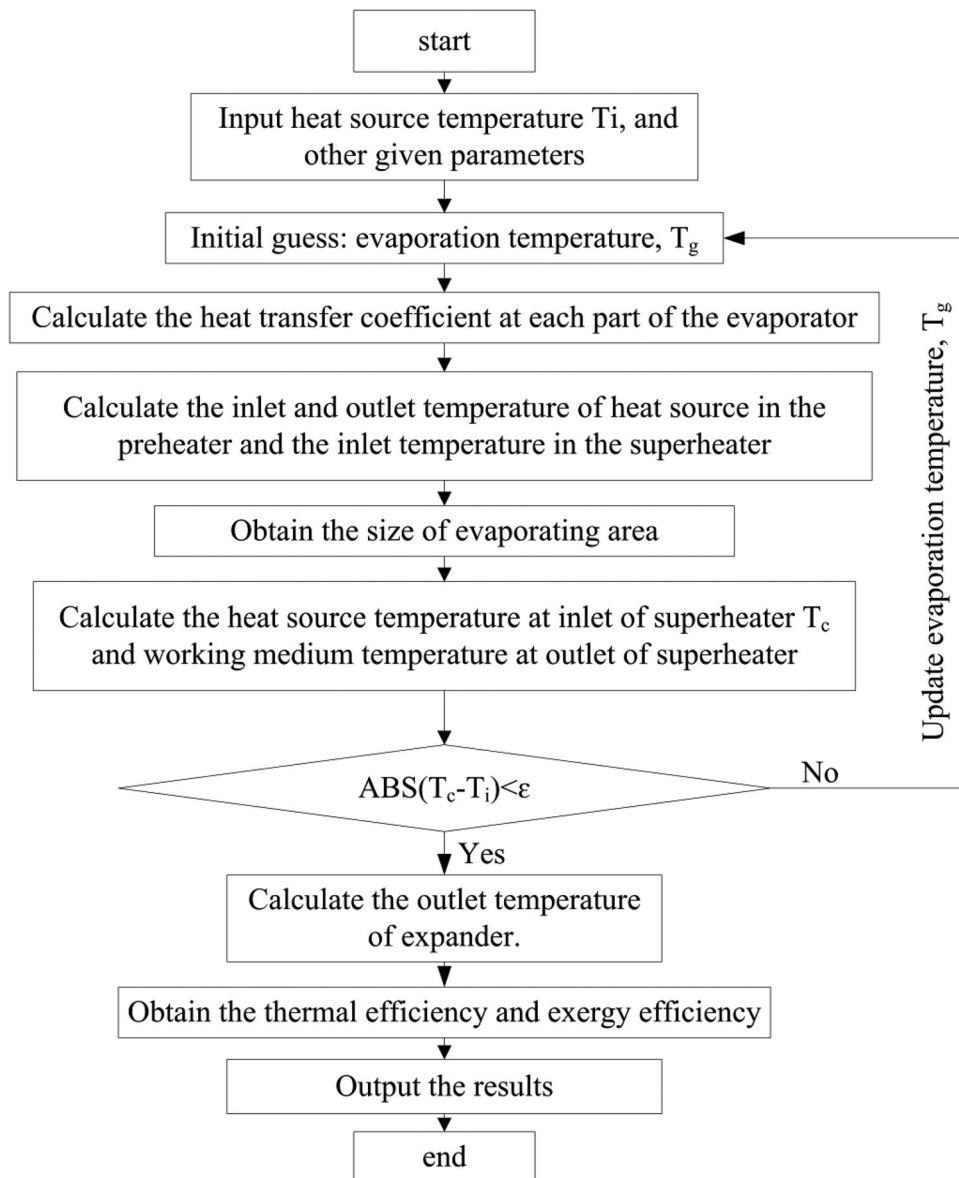


Figure 4. Flow chart of evaporator module.

(preheating area size F_j and superheating area F_k), the heat source inlet temperature and mass flow rate, the inlet state of the working medium and the working medium mass flow rate. Based on the aforementioned equations, an iterative method is established here to determine the outlet states of the heat source and working medium and the thermal efficiency of the system under the given operating conditions. The detailed procedures in the simulation model are summarized as follows:

1. Input the given parameters in both the heat source and working medium sides and assume the evaporating temperature.
2. Calculate heat transfer coefficient in preheating area (Eqs. 1 and 3–4).
3. Calculate the heat source outlet and inlet temperature in the preheater and heat source temperature at inlet of superheater (Eqs. 5–6).
4. Divide evaporating area into ten segments as shown in Figure 3, and calculate the convective heat transfer coefficient for each segment and obtain the heat transfer of evaporating area (Eqs. 2 and 4).
5. Obtain the size of evaporating area (Eq. 6).
6. Calculate the heat source inlet temperature of superheater (Eqs. 3–6).
7. Resume the model with an updated guess of the evaporating temperature until the difference between the given heat source temperature and calculated value is within the allowable error.

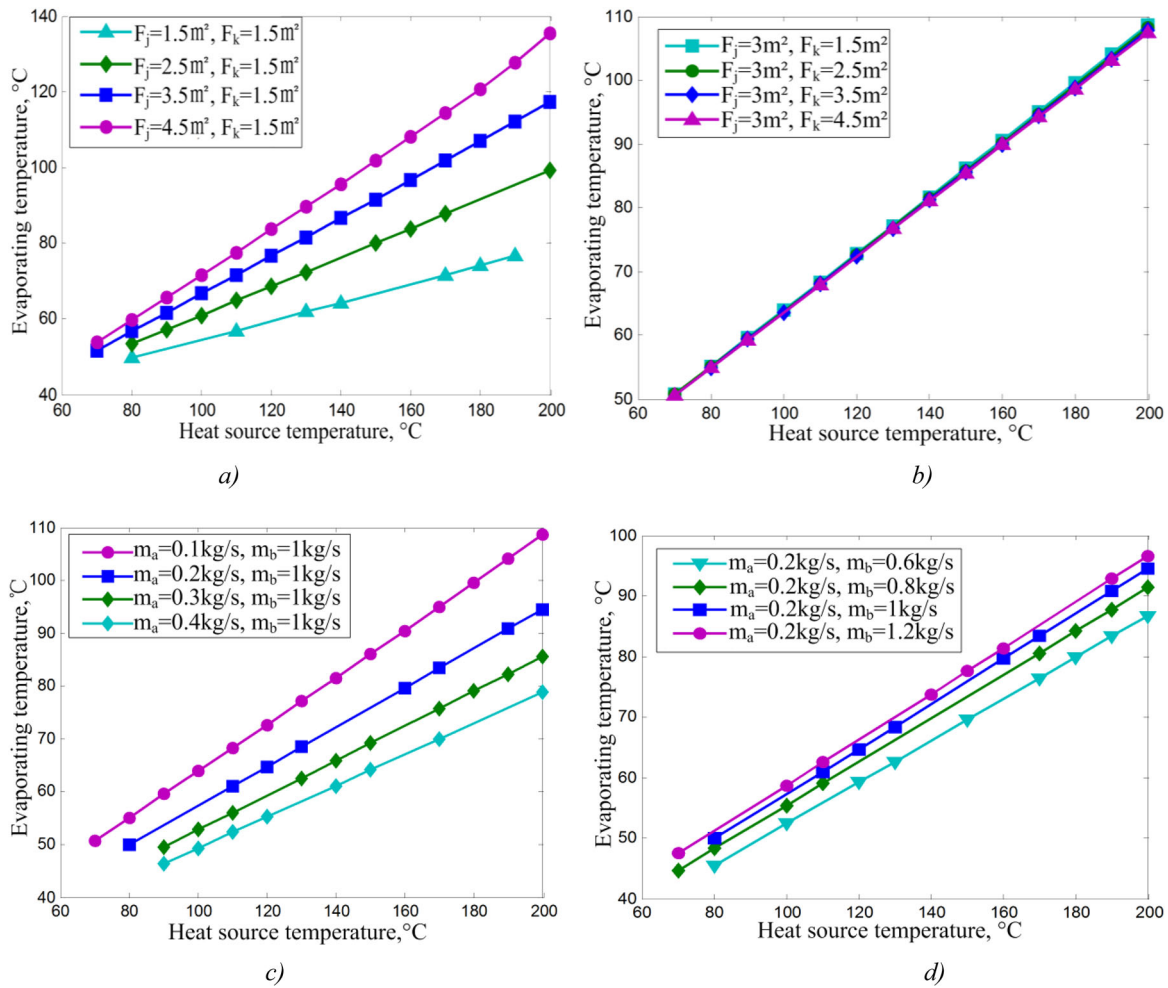


Figure 5. Relationships between evaporating temperature and the heat source temperature under different operating conditions.

8. Obtain the outlet parameters of expander and calculate output power of expander and input power of medium heat pump (Eqs. 8–10).
9. Calculate the heat transfer rate in the evaporator and the system efficiency (Eqs. 7 and 11).
10. Calculate the exergy losses and exergy efficiency of the evaporator (Eqs. 12–15).

The flow chart of the system is expressed in Figure 4.

Results and discussion

The design modeling procedure requires a set of parameters that are specific to each ORC system, such as the properties of the heat source, the design of the heat exchanger and the operation of the heat pump. All of these parameters affect the performance of the ORC system to some extent, but the flow rate of the heat source and working medium, the temperature of the heat source and the configuration of the heat

exchanger are the most important factors. In discussing the influence of these parameters on the performance of the ORC system, the following parameters are defined as design benchmarks.

The evaporator of the system applies the double-pipe heat exchanger, the diameter and thickness of the inner pipe are 104 and 2 mm, respectively, and diameter of the outer pipe is 228 mm. The thermal conductivity of the heat exchanger is $46 \text{ W} \cdot \text{m}^{-1} \cdot \text{K}^{-1}$. The condensing temperature is designed at 43°C , and does not vary as the other parameters change. To investigate the impact of the flow rate, heat exchanger configuration and heat source temperature on the efficiency of the system, each parameters is changed, respectively, for comparison.

Analysis of the evaporator size and evaporating temperature

In this study the impacts of the preheating and superheating areas and fluid flow rates on the evaporator

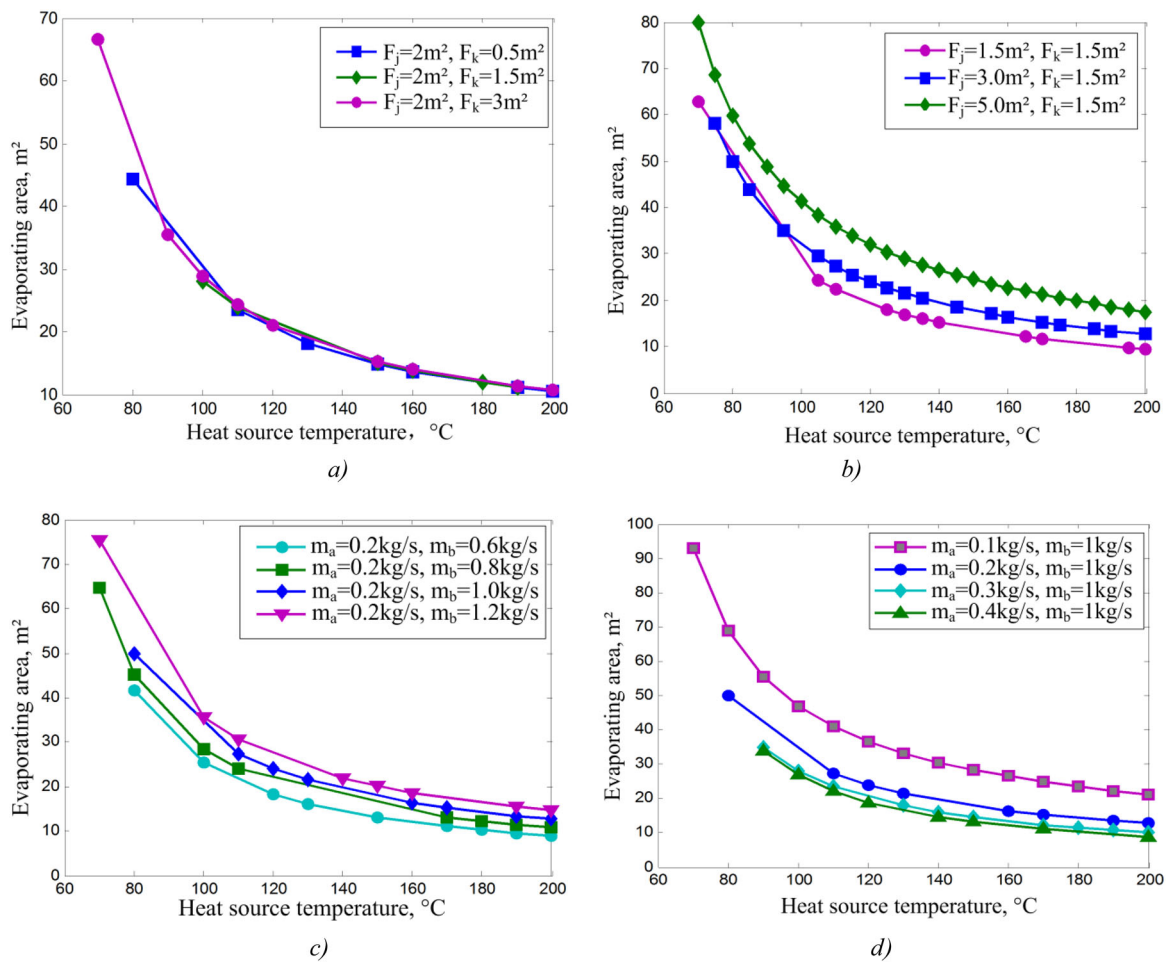


Figure 6. Relationships between evaporating area of the heat exchanger and the heat source temperature under different operating conditions.

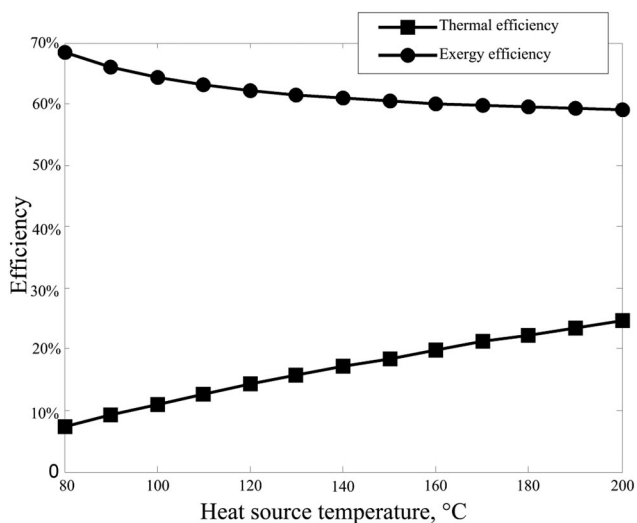


Figure 7. Variation of the system thermal efficiency and evaporator exergy efficiency as heat source temperature increases.

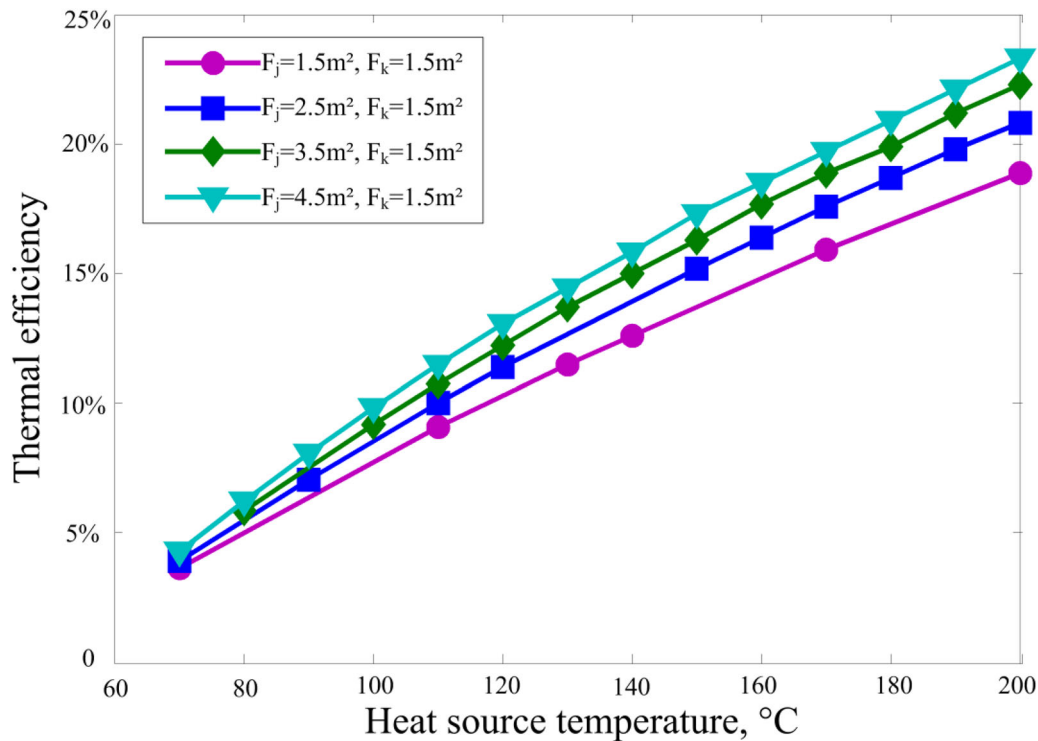
size and evaporating temperature are investigated. It is found when the preheater area varies from 1.5 to 4.5 m², the evaporating temperatures vary a lot and

show an obvious increasing trend, but when the superheater area rises from 1.5 to 4.5 m², the curves of evaporating temperatures are almost the same. That means enlarging preheater area can raise evaporating temperature, while the superheater area has little impact on evaporating temperature as is shown in a) and b) in Figure 5.

As the heat source temperature rises from 80 to 200 °C, the evaporating temperature has a linear increase. When the flow rate of the working fluid varies from 0.1 to 0.4 kg/s, the evaporating temperature has certain decreases, but the growth rate of evaporating temperature drops slowly as working fluid flow rate increases. However when the flow rate of the working fluid is constant, the heat source flow rate varies from 0.6 to 1.2 kg/s, the evaporating temperature increases but just in a small scale. The curve in c) and d) in Figure 5 suggests it is beneficial to increase evaporating temperature by enlarging heat source flow rate or reducing working fluid flow rate, and reducing the working fluid flow rate is a more efficient way.

Table 2. Parameters of different parts of the ORC system for each case, when the temperature of the heat source rises from 80 to 200 °C.

Heat source temperature °C	Heat source outlet temperature °C	Preheater inlet temperature °C	Evaporating temperature °C	Superheater outlet temperature °C	Expander outlet temperature °C	System heat efficiency	Exergy efficiency of the evaporator
80	71	43	51	53.7	44.5	7.3%	68.4%
100	91.4	43	58.6	68.7	45.2	10.8%	64%
120	109.9	43	66.0	84.6	46.0	14.2%	62%
140	129.4	43	75.1	99.8	47.6	17.1%	61%
160	148.9	43	83.9	113.7	48.51	19.9%	60%
180	168.3	43	92.1	123.7	49.38	22.2%	59.3%
200	187.3	43	99.1	130.9	50.11	24.6%	59%

**Figure 8.** Thermal efficiency variation of the system as the preheater area varies from 1.5 to 4.5 m².

As the heat source temperature increases from 80 to 200 °C, there is a sharp decline in evaporating area. That is because as the evaporating temperature rises, the enthalpy difference between the inlet of evaporator and outlet evaporator is reduced. That means the fluid absorbs less heat to get into the superheater, while the temperature difference between the heat source and working fluid enlarges as the heat source temperature rises, so smaller evaporating area is required to absorb enough heat for the working fluid. It is also found in this paper, the change of superheater area has a weak impact on the evaporating area, while the increase of the preheating area makes an obvious increase on the evaporating area as is shown in a) and b) of Figure 6.

As to the impact of the flow rate on the evaporating area, it can be known in c) and d) in Figure 6, both the increase of the heat source and the decrease of the working fluid decrease the evaporating area

efficiently, but the impact of the working fluid decreases with the increase of the working fluid rate. That is because the larger difference flow rate of the heat source and working fluid causes more efficient heat transfer in the evaporator. As the flow rate difference reduces, and its impact on the heat transfer efficiency is reduced, so that the evaporating area variation becomes less obvious. So in the real project, enlarging the flow rate between heat source medium and working fluid medium or increasing preheater area appropriately can reduce the evaporating area, and save heat exchanger cost.

Thermal analysis of the designed system

In the computer model, in order to investigate the impacts of the heat source temperature on the system thermal efficiency and evaporator exergy efficiency,

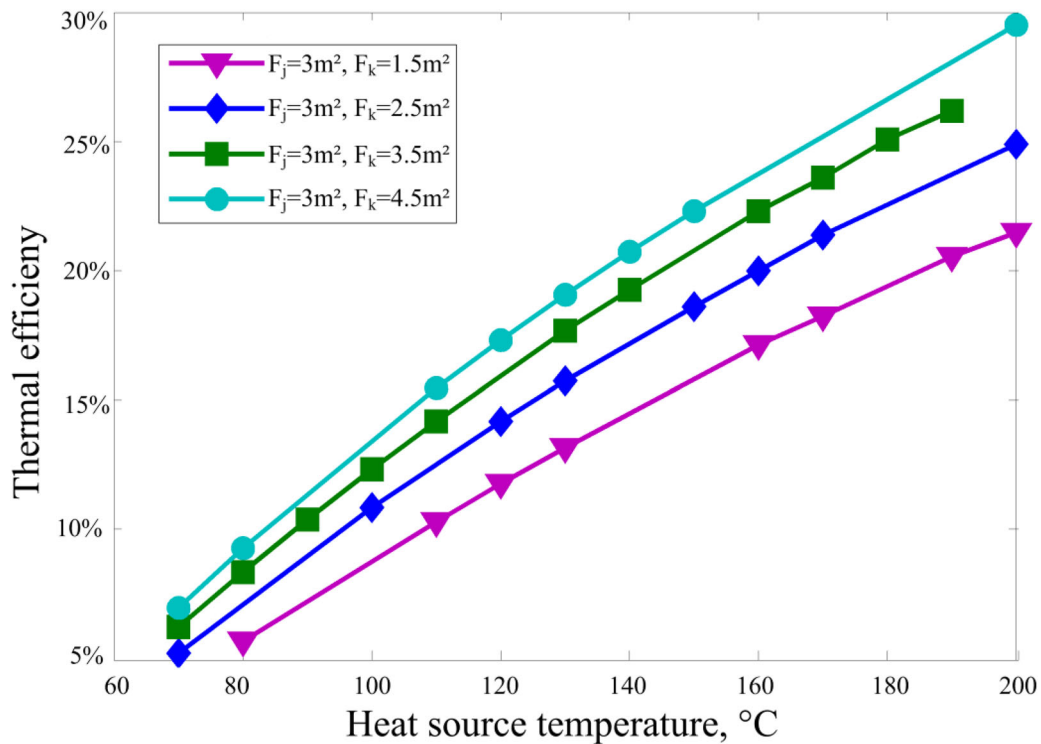


Figure 9. Thermal efficiency variation of the system as the superheater area varies from 1.5 to 4.5 m².

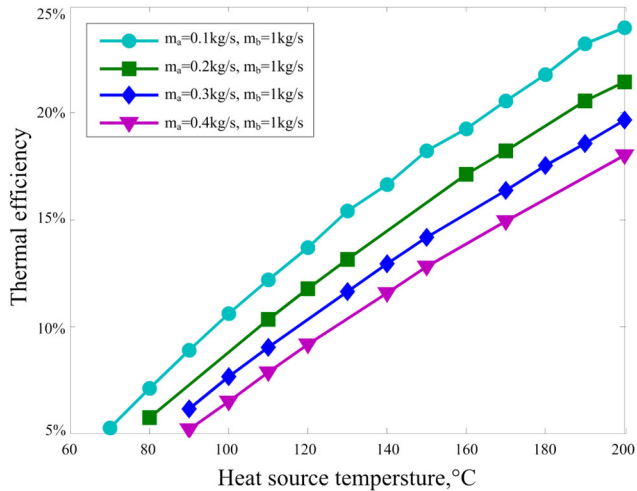


Figure 10. Thermal efficiency variation of the system as the medium flow rate varies from 0.1 to 0.4 kg/s.

the preheater and the superheater areas are, respectively, set at 3.5 and 1.5 m², and the flow rates of waste heat and working medium are respectively set at 1 and 0.1 kg/s. It can be found in Figure 7 and Table 2, the thermal efficiency of the system increases from 8% to 24% when the heat source temperature increases from 80 to 200 °C. while the exergy efficiency of the evaporator decreases from 69% to 59% with the increase of the heat source temperature. This is because the increase of the heat source temperature

enlarges the average temperature difference between the heat source and working fluid, and higher temperature difference results in more irreversible loss. The degree of the irreversible heat loss increasing is comparatively higher than that of the exergy input increasing, so the exergy efficiency decreases. In addition, high heat source temperature enlarges the evaporating temperature and the evaporator outlet ORC fluid enthalpy, but the degree of the increase is comparatively higher than that of the increase of the heat absorbed by the evaporator, so the thermal efficiency increases.

Because the evaporator is designed into three parts (preheating zone, evaporating zone and superheating zone), the impact of the evaporator on the performance of the system is investigated by controlling the preheater area and superheater area. Figure 8 explains that the area of the preheater increases from 1.5 to 4.5 m² when the area of the superheater is constant, and therefore the thermal efficiency of the system increases in a small scale. That means when the superheater area is 1.5 m², the variation of the preheater area has a weak impact on the performance of the system; but when the preheater area is designed to be constant as shown in the Figure 9, as the superheater area varies from 1.5 to 4.5 m², the variation of thermal efficiency causes an obvious increase, but the growth rate decreases with the increase of the superheater area. This is because the specific heat of

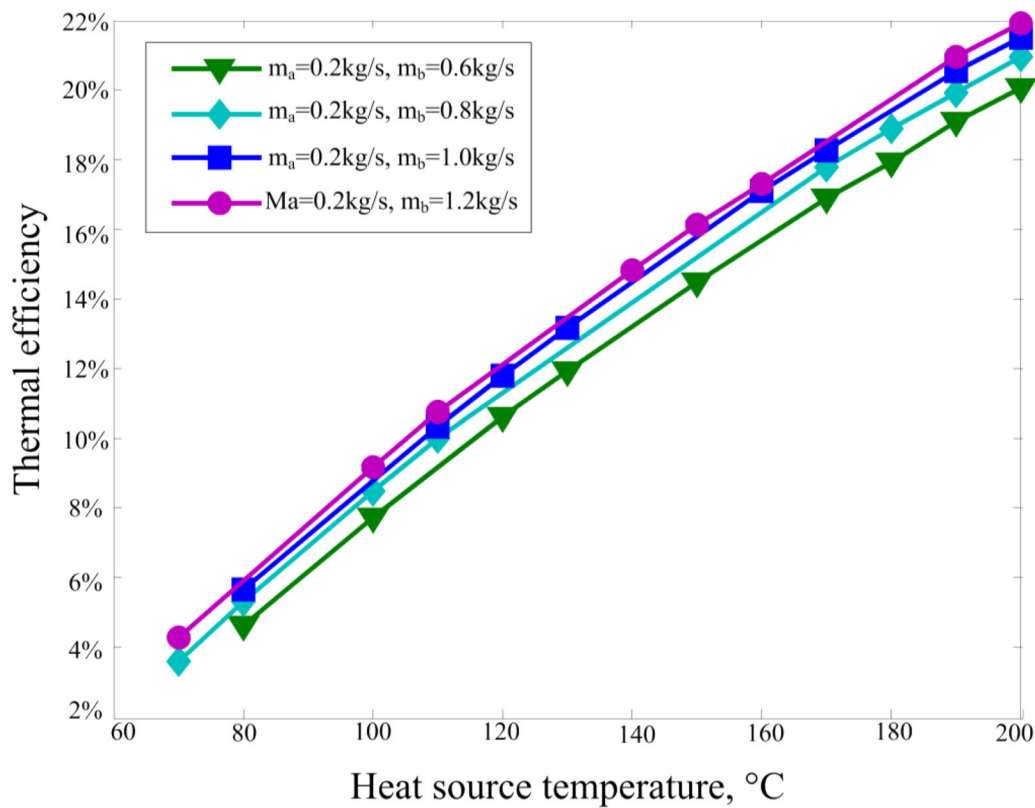


Figure 11. Thermal efficiency variation of the system as the waste source flow rate varies from 0.6 to 1.2 kg/s.

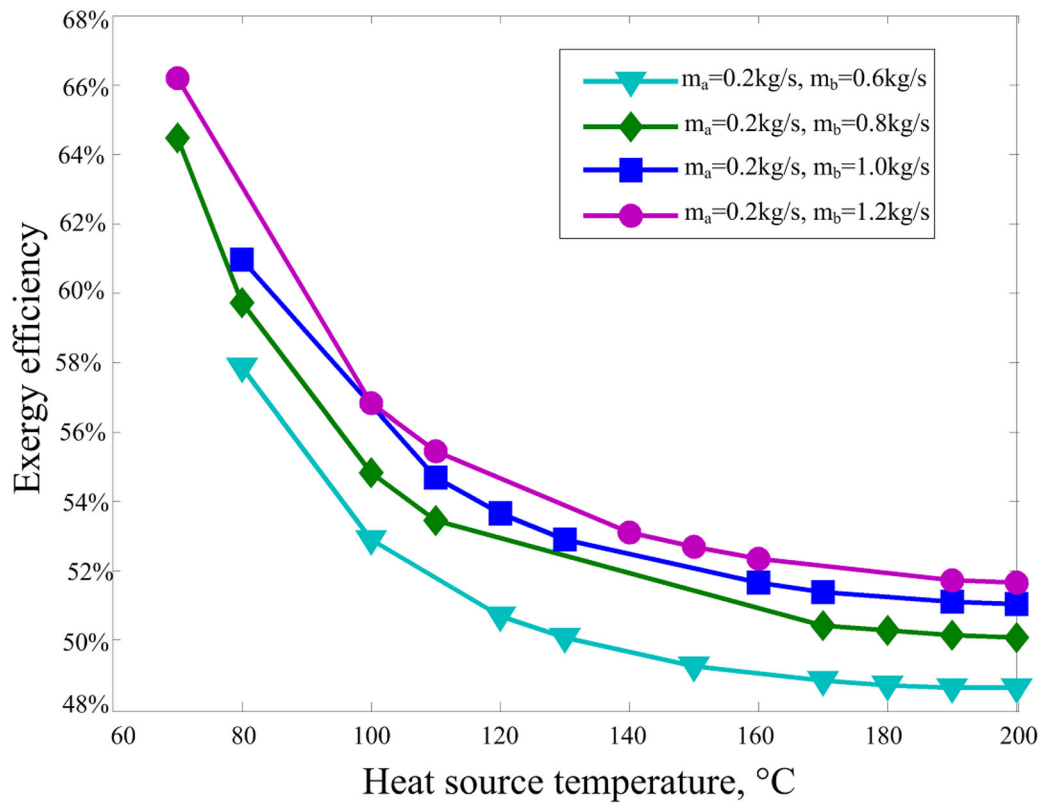


Figure 12. Exergy efficiency variation of the evaporator as the heat source flow rate varies from 0.6 to 1.2 kg/s.

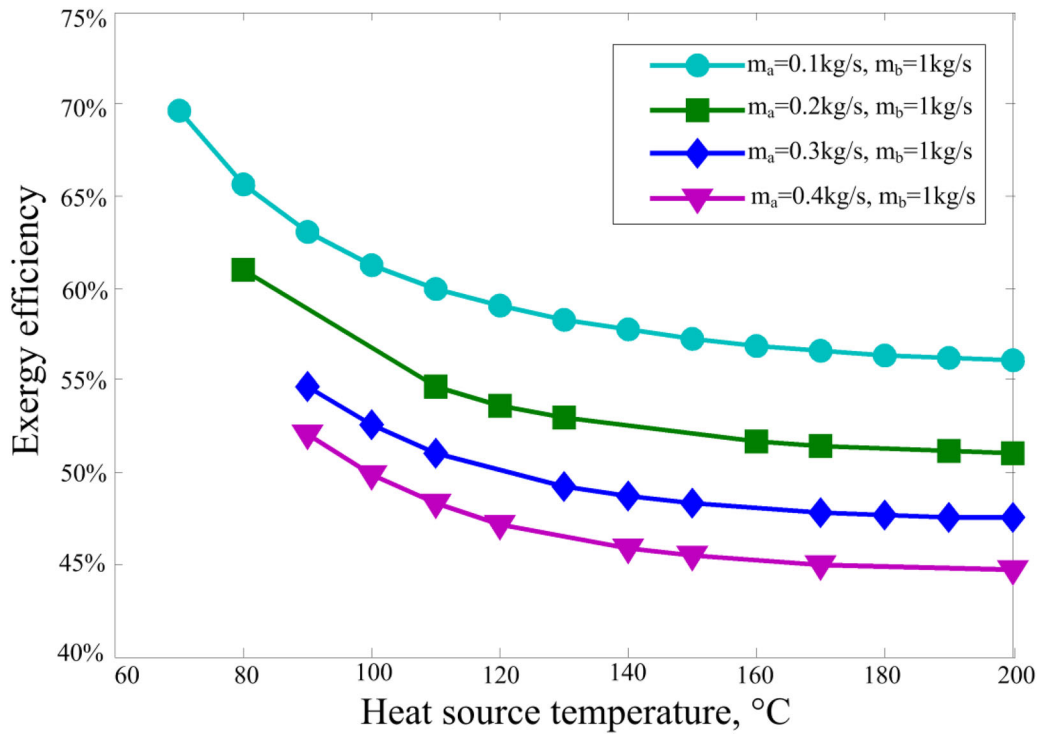


Figure 13. Exergy efficiency variation of the evaporator as the medium flow rate varies from 0.1 to 0.4 kg/s.

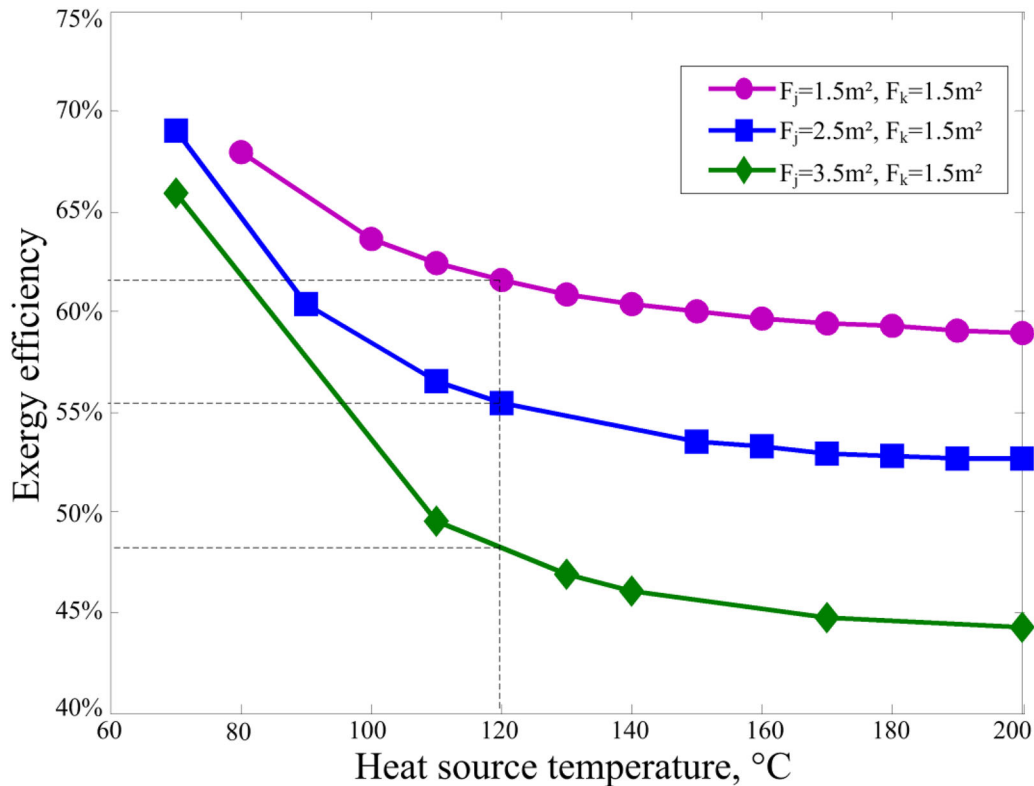


Figure 14. Exergy efficiency variation of the evaporator as the transfer area of the preheater varies from 1.5 to 3.5 m².

overheated refrigerant increases with the temperature increases. When the preheater area is enlarged, the refrigerant temperature at inlet of the evaporator increases. But the refrigerant temperature at the outlet

of superheater increases in a small scale because of the increase of overheated refrigerant specific heat. And the inlet temperature is constant at 43 °C, so the increase of the preheater area enlarges the temperature

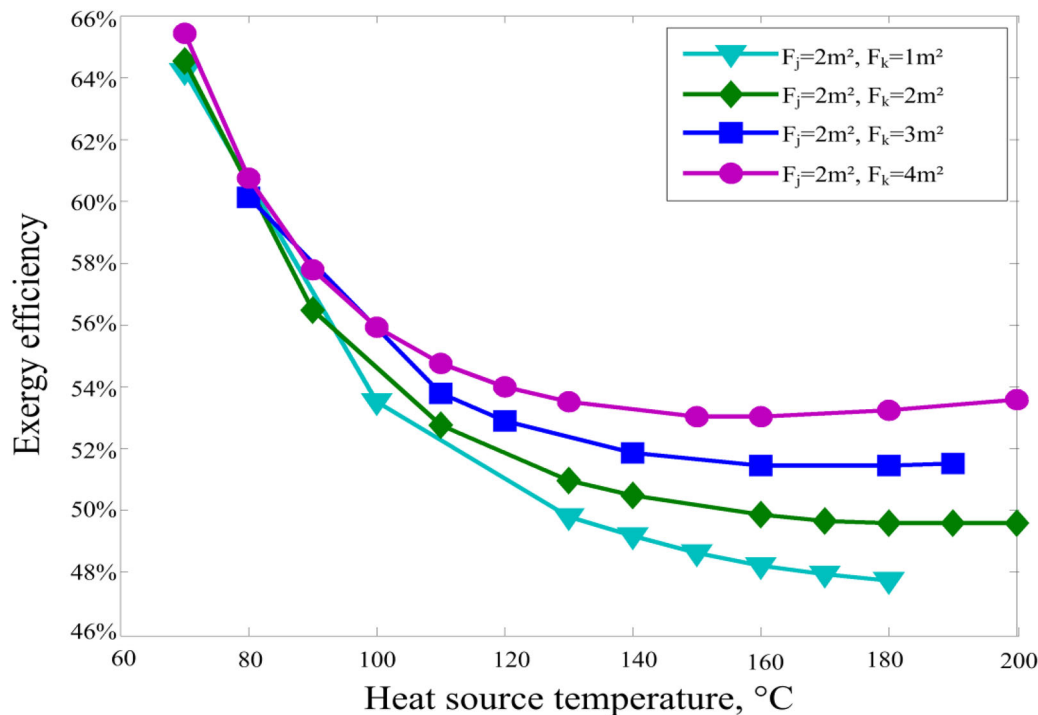


Figure 15. Exergy efficiency variation of the evaporator as the transfer area of the superheater varies from 1 to 4 m².

difference between heat source and working fluid, so the inlet temperature of the evaporator and outlet temperature of the superheater is almost constant, and the efficiency has a weak variation; but the increase of the superheater area leads the decrease of the temperature difference between the heat source and working fluid, so the outlet temperature of the superheater increases obviously and the efficiency behaves an obvious variation. As shown in Figure 10, when the temperature of the heat source rises from 80 to 200 °C and the flow rate of the heat source is constant, the system thermal efficiency increases respectively, and as the flow rate of the working medium increases from 0.1 to 0.4 kg/s, the system thermal efficiency drops to a certain extent. However, as shown in Figure 11, when the working medium flow rate is constant, the efficiency variation is not obvious with the increase of the heat source flow rate, which means the working medium flow rate has a more effective influence on the system. This is because when the flow rate of the working medium is 0.2 kg/s, it absorbs less heat to reach high temperature, but when the heat source flow rate varies, the heat transferred to the medium is almost constant, so the efficiency does not vary a lot.

Exergy analysis of the designed system

In this model, it is found that in Figure 12, when the temperature rises from 80 to 200 °C, the exergy efficiency is similarly constant for the system with the

heat source flow rate of 0.6 kg/s. It can also be obtained when the flow rate of the waste oil increases, the efficiency increases rapidly but declines obviously with the increase of the temperature. The reason is when the flow rate of the heat source increases, the temperature difference between the heat source and working fluid is reduced, so the exergy losses are decreased and exergy efficiency increases. However, when the working medium flow rate rises to a certain extent, the exergy efficiency dropped relatively, the efficiency declines from 70 to 55.9% while the flow rate is 0.1 kg/s. This is because as the temperature of the heat source increases, the temperature gap between the heat source and working fluid is enlarged. That leads to the the increase of exergy losses, so that exergy efficiency decreases. Figure 13 exhibits that the efficiency declines from 53 to 46% if the flow rate is 0.4 kg/s.

Figure 14 shows that the size of the preheater increases from 1.5 to 3.5 m² and the exergy efficiency decreases from 57 to 44% when the heat source temperature is 120 °C. As the heat source temperature increases, bigger area of the preheater leads to the quicker efficiency decrease, which decreases from 61 to 39% for the area is 3.5 m², but for a system with superheating area of 1.5 m² it has just 9% efficiency decrease which is from 64 to 55%. The reason is when the heat source temperature is constant, as the increase of the preheater area, more heat will be transferred to the working fluid from the heat source,

leading to the decrease of the average temperature difference between the heat source and working fluid, so the exergy losses decrease. When the preheater area is constant, as the increase of the heat source temperature, the average temperature difference is enlarged, so the exergy efficiency decreases. As to the larger area of the preheater, as the temperature rises, the outlet temperature of the evaporator increases more and more slowly, causing the quicker decrease of the exergy efficiency.

When the heat source temperature increases from 80 to 200 °C, the superheater area increases from 1 to 4 m², the exergy efficiency of the evaporator decreases, respectively; but the degrees of the decrease are different. Figure 15 illustrates that a superheating area of 4m² is adopted in the system and thus the exergy efficiency declined from 65 to 55%. This fall range is slower than that of the system with a declining degree of from 65 to 48% while a superheating area of 1 m² is used. Accordingly, the larger superheating area is beneficial to reduce the exergy losses in the evaporator.

Conclusions

In this study, a simulation model of the ORC power generating system is developed, and this system employs R245fa as the working medium and is driven by the waste oil from the industry mills. According to the parameters of the ORC system in different cases, the relevant parameters can be worked out. It is a good reference for ORC system design and evaporator design.

The study has shown that evaporating temperature and evaporating area of evaporator are affected a lot by the superheater area and working medium flow rate. When the heat source temperature is designed at 200 °C, evaporating temperature increases from 80 to 140 °C, as preheater area increases from 1.5 to 4.5 m². As to the evaporating area, when working fluid flow rate decreases from 0.4 to 0.1 kg/s, evaporating area decreases from 28 to 10 m², and at the same time the thermal efficiency rises from 17 to 24%.

The system thermal efficiency and exergy efficiency of the evaporator are analyzed by this model. By giving different flow rates of working medium and areas of the evaporator, the performance of the system is analyzed. It is found that adding the superheater area or increasing the flow rate difference between working medium and heat source is efficient way to increase the thermal efficiency of the system under the proper condition.

It can be understood from the simulation model, the parameters of the evaporator, working medium and the heat source have significant influence on the performance of the ORC power generating system. The model is a good foundation for the further research on the optimization on the ORC power generating system.

Funding

The work described in this paper was supported by a Grant from Shandong Key R&D Program (No. 2017GGX40117), and supported by a Grant from National Natural Science Foundation of China (Project No. 5170 8336).

Notes on contributors



Xinlei Zhou is a second year master student at the School of Thermal Engineering of Shandong Jianzhu University. His main research interests are in the field of sustainable energy technologies. He has been focused on research on the industrial waste heat recovery for 2 years and has published two papers in refereed journals.



Ping Cui is an Associate Professor of the School of Thermal Engineering of Shandong Jianzhu University. She obtained her PhD degree in the field of renewable energy applications in buildings from The Hong Kong Polytechnic University. Her main research interests are in building energy management and sustainable energy technologies. She has focused on the study and application of the ground source heat pump technologies since 1999. Now she is conducting the study on the technology of the combination of ground thermal energy and solar energy for building HVAC system. She was/is involved over twelve research and technology development funds from national and local government, and industrial funds. She has published around 40 papers in refereed journals.



Wenke Zhang is a lecturer of the School of Thermal Engineering of Shandong Jianzhu University. His main research areas include heat transfer and ground source heat pump. He obtained the PhD degree

from The Hong Kong Polytechnic University. He has published more than 20 high level papers in journals, and take charge of National and Provincial scientific research projects.

References

1. L. Wang, A. P. Roskilly, and R. Wang, "Solar powered cascading cogeneration cycle with ORC and adsorption technology for electricity and refrigeration," *Heat Transfer Eng.*, vol. 35, no. 11–12, pp. 1028–1034, 2014. DOI: [10.1080/01457632.2013.863067](https://doi.org/10.1080/01457632.2013.863067).
2. Y. Dai, D. Hu, Y. Wu, Y. Gao, and Y. Cao, "Comparison of a basic organic Rankine cycle and a parallel double-evaporator organic Rankine cycle," *Heat Transfer Eng.*, vol. 38, no. 11–12, pp. 990–999, 2017. DOI: [10.1080/01457632.2016.1216938](https://doi.org/10.1080/01457632.2016.1216938).
3. F. Velez, "A technical, economical and market review of organic Rankine cycles for the conversion of low-grade heat for power generation," *Renew. Sustain. Energy Rev.*, vol. 16, no. 3, pp. 4175–4189, 2012.
4. S. Quoilin, M. V. D. Broek, S. Declaye, P. Dewallef, and V. Lemort, "Techno-economic survey of organic Rankine cycle (ORC) systems," *Renew. Sustain. Energy Rev.*, vol. 22, no. 1, pp. 168–186, 2013. DOI: [10.1016/j.rser.2013.01.028](https://doi.org/10.1016/j.rser.2013.01.028).
5. B. F. Tchanche, M. Pétrissans, and G. Papadakis, "Heat resources and organic Rankine cycle machines," *Renew. Sustain. Energy Rev.*, vol. 39, pp. 1185–1199, 2014. DOI: [10.1016/j.rser.2014.07.139](https://doi.org/10.1016/j.rser.2014.07.139).
6. M. Z. Stijepovic, *et al.*, "Organic Rankine cycle system performance targeting and design for multiple heat sources with simultaneous working fluid selection," *J. Clean. Prod.*, vol. 142, no. 11, pp. 1950–1970, 2017. DOI: [10.1016/j.jclepro.2016.11.088](https://doi.org/10.1016/j.jclepro.2016.11.088).
7. R. Mathie, C. N. Markides, and A. J. White, "A framework for the analysis of thermal losses in reciprocating compressors and expanders," *Heat Transfer Eng.*, vol. 35, no. 16–17, pp. 1435–1449, 2014. DOI: [10.1080/01457632.2014.889460](https://doi.org/10.1080/01457632.2014.889460).
8. C. He *et al.*, "A new selection principle of working fluids for subcritical organic Rankine cycle coupling with different heat sources," *Energy*, vol. 68, no. 2, pp. 283–291, 2014. DOI: [10.1016/j.energy.2014.02.050](https://doi.org/10.1016/j.energy.2014.02.050).
9. J. S. Brown, R. Brignoli, and T. Quine, "Parametric investigation of working fluids for organic Rankine cycle applications," *Appl. Therm. Eng.*, vol. 90, no. 6, pp. 64–74, 2015. DOI: [10.1016/j.applthermaleng.2015.06.079](https://doi.org/10.1016/j.applthermaleng.2015.06.079).
10. J. Song, C. Gu, and X. Li, "Performance estimation of tesla turbine applied in small scale organic Rankine cycle (ORC) system," *Appl. Therm. Eng.*, vol. 110, no. 8, pp. 318–326, 2017. DOI: [10.1016/j.applthermaleng.2016.08.168](https://doi.org/10.1016/j.applthermaleng.2016.08.168).
11. V. Lemort, S. Quoilin, C. Cuevas, and J. Lebrun, "Testing and modeling a scroll expander integrated into an organic Rankine cycle," *Appl. Therm. Eng.*, vol. 29, no. 14–15, pp. 3094–3102, 2009. DOI: [10.1016/j.applthermaleng.2009.04.013](https://doi.org/10.1016/j.applthermaleng.2009.04.013).
12. T. Yamamoto, T. Furuhashi, N. Arai, and K. Mori, "Design and testing of the organic Rankine cycle," *Energy*, vol. 26, no. 3, pp. 239–251, 2001. DOI: [10.1016/S0360-5442\(00\)00063-3](https://doi.org/10.1016/S0360-5442(00)00063-3).
13. G. Pei, J. Li, Y. Li, D. Wang, and J. Ji, "Construction and dynamic test of a small-scale organic Rankine cycle," *Energy*, vol. 36, no. 5, pp. 3215–3223, 2011. DOI: [10.1016/j.energy.2011.03.010](https://doi.org/10.1016/j.energy.2011.03.010).
14. S. H. Kang, "Design and experimental study of ORC (organic Rankine cycle) and radial turbine using R245fa working fluid," *Energy*, vol. 4, no. 5, pp. 514–524, 2012. DOI: [10.1016/j.energy.2012.02.035](https://doi.org/10.1016/j.energy.2012.02.035).
15. A. Kaya, M. Lazova, Ö. Bağcı, S. Lecompte, B. Ameer, and M. De Paepe, "Design sensitivity analysis of a plate-finned air-cooled condenser for low-temperature organic Rankine cycles," *Heat Transfer Eng.*, vol. 38, no. 11–12, pp. 1018–1033, 2017. DOI: [10.1080/01457632.2016.1216966](https://doi.org/10.1080/01457632.2016.1216966).
16. T. Sung, *et al.*, "Performance characteristics of a 200-kW organic Rankine cycle system in a steel processing plant," *Appl. Energy*, vol. 183, no. 9, pp. 623–635, 2016. DOI: [10.1016/j.apenergy.2016.09.018](https://doi.org/10.1016/j.apenergy.2016.09.018).
17. Z. Miao, J. Xu, X. Yang, and J. Zou, "Operation and performance of a low temperature organic Rankine cycle," *Appl. Therm. Eng.*, vol. 75, pp. 1065–1075, 2015. DOI: [10.1016/j.applthermaleng.2014.10.065](https://doi.org/10.1016/j.applthermaleng.2014.10.065).
18. B.-R. Fu, S.-W. Hsu, Y.-R. Lee, J.-C. Hsieh, C.-M. Chang, and C.-H. Liu, "Effect of off-design heat source temperature on heat transfer characteristics and system performance of a 250-kW organic Rankine cycle system," *Appl. Therm. Eng.*, vol. 70, no. 1, pp. 7–12, 2014. DOI: [10.1016/j.applthermaleng.2014.04.065](https://doi.org/10.1016/j.applthermaleng.2014.04.065).
19. R. J. Xu and Y. L. He, "A vapor injector-based novel regenerative organic Rankine cycle," *Appl. Therm. Eng.*, vol. 31, no. 6–7, pp. 1238–1243, 2011. DOI: [10.1016/j.applthermaleng.2010.12.026](https://doi.org/10.1016/j.applthermaleng.2010.12.026).
20. A. I. Papadopoulos, M. Stijepovic, and P. Linke, "On the systematic design and selection of optimal working fluids for organic Rankine cycles," *Appl. Therm. Eng.*, vol. 30, no. 6–7, pp. 760–769, 2010. DOI: [10.1016/j.applthermaleng.2009.12.006](https://doi.org/10.1016/j.applthermaleng.2009.12.006).
21. H. Wang, H. Wang, and E. Long, "Parameter optimization of the low-temperature exhaust gas waste heat powered organic Rankine cycle," *J. Iron Steel Res. Int.*, vol. 29, no. 3, pp. 1183–1189, 2009.
22. N. Mashoofi, S. Pourahmad, and S. M. Pesteei, "Study the effect of axially perforated twisted tapes on the thermal performance enhancement factor of a double tube heat exchanger," *Case Stud. Therm. Eng.*, vol. 10, pp. 161–168, 2017. DOI: [10.1016/j.csite.2017.06.001](https://doi.org/10.1016/j.csite.2017.06.001).